0026-895X/09/7501-134–142$20.00
MOLECULAR PHARMACOLOGY
Vol. 75, No. 1
50567/3414483
Mol Pharmacol 75:134–142, 2009
Printed in U.S.A.

Thiophenecarboxylate Suppressor of Cyclic Nucleotides Discovered in a Small-Molecule Screen Blocks Toxin-Induced Intestinal Fluid Secretion[S]

Lukmanee Tradtrantip, Buranee Yangthara, Prashant Padmawar, Christopher Morrison, and A. S. Verkman

Departments of Medicine and Physiology, Cardiovascular Research Institute, University of California, San Francisco, California

Received July 14, 2008; accepted September 25, 2008

ABSTRACT

We carried out a "pathway" screen of 50,000 small molecules to identify novel modulators of cAMP signaling. One class of compounds, the 2-(acylamino)-3-thiophenecarboxylates, strongly suppressed cAMP and cGMP in multiple cell lines in response to different agonists acting on G-protein-coupled receptors, adenylyl cyclase, and guanylyl cyclase. The best compounds from structure-activity analysis of 124 analogs, including several synthesized chiral analogs, had and IC_{50} of <5 μM for suppression of agonist-induced cAMP and cGMP elevation. Measurements of cAMP, cGMP, and downstream signaling in response to various activators/inhibitors suggested that the 2-(acylamino)-3-thiophenecarboxylates function as nonselective phosphodiesterase activators, although it was not determined whether their action on phosphodiesterases is direct or indirect. The 2-(acylamino)-3-thiophenecarboxylates suppressed CFTR-mediated Cl^- current in T84 colonic cells in response to cholera and *Escherichia coli* (STa) toxins, and prevented intestinal fluid accumulation in a closed-loop mouse model of secretory diarrhea. They also prevented cyst growth in an in vitro renal epithelial cell model of polycystic kidney disease. The 2-(acylamino)-3-thiophenecarboxylates represent the first small-molecule cyclic nucleotide suppressors, whose potential therapeutic indications include secretory diarrheas, polycystic kidney disease, and growth inhibition of cAMP-dependent tumors.

Cyclic AMP (cAMP) signaling is of central importance in the regulation of cell growth, ionic composition and volume, as well as in specialized tissue functions such as transepithelial fluid secretion and absorption, and muscle contraction (Meyer et al., 2005; Murthy, 2006; van Staveren et al., 2006). Pathological elevation in cAMP as a result of toxins, hormonal imbalance or G-protein mutations is involved in the pathogenesis of enterotoxin-mediated secretory diarrheas (Sack et al., 2004), polycystic kidney disease (Sweeney and Avner, 2006), and certain adenomas and other tumors (Murakami et al., 1999). Cytoplasmic cAMP concentration is determined primarily by the rates of cAMP generation and degradation, which depend on adenylyl cyclase and phosphodiesterase (PDE) activities, respectively. The related cyclic nucleotide cGMP, which is involved in smooth muscle contraction and some types of secretory diarrheas (Vaandrager, 2002; Rybalkin et al., 2003), is generated by guanylyl cyclase and degraded by a subset of PDEs. Drugs that increase cyclic nucleotide concentrations have proven utility in a various conditions, such as heart failure and asthma (cAMP activators) and pulmonary hypertension and erectile dysfunction (cGMP activators). In theory, drugs that reduce cyclic nucleotide concentration may be of potential utility in a different set of conditions, including secretory diarrheas, polycystic kidney disease, and tumor growth.

The original goal of this study was to identify, using a cAMP "pathway" screen, novel small-molecule inhibitors of the vasopressin-2 receptor, Gs-type G-protein, protein kinase A, and cystic fibrosis transmembrane conductance regulator (CFTR) protein. In our pathway screen, as diagrammed in

This work was supported by grants DK72517, DK35124, HL59198, EY13574, EB00415, and HL73856 from the National Institutes of Health, and Research Development Program (R613) and Drug Discovery grants from the Cystic Fibrosis Foundation.

Article, publication date, and citation information can be found at http://molpharm.aspetjournals.org.

doi:10.1124/mol.108.050567.

[S] The online version of this article (available at http://molpharm.aspetjournals.org) contains supplemental material.

ABBREVIATIONS: PDE, phosphodiesterase; CFTR, cystic fibrosis transmembrane conductance regulator; V_2R, vasopressin-V2 receptor; dDAVP, desmopressin; CTX, cholera toxin; STa, *Escherichia coli* heat-stable toxin; CPT, chlorophenylthio; IBMX, 3-isobutyl-1-methylxanthine; FRT, Fisher rat thyroid; YFP, yellow fluorescent protein; MDCK, Madin-Darby canine kidney; CHO, Chinese hamster ovary; PBS, phosphate-buffered saline; DMSO, dimethyl sulfoxide; ES-MS, electrospray mass spectroscopy; MRP, multidrug resistance protein; PDE, phosphodiesterase; CNT, cyclic nucleotide.

Fig. 1A, activation of CFTR Cl^- conductance by protein kinase A-mediated CFTR phosphorylation serves as read-out for vasopressin-induced cAMP elevation. The screen produced a novel class of vasopressin-V2 receptor (V_2R) antagonists, as reported previously (Yangthara et al., 2007): several CFTR inhibitors of chemical classes identified previously from a target-based screen (Ma et al., 2002; Muanprasat et al., 2004) and a class of 2-(acylamino)-3-thiophenecarboxylates as reported in this article. We found that the 2-(acylamino)-3-thiophenecarboxylates suppressed cellular cAMP and cGMP in different cell lines and in response to different types of agonists and seem to function as PDE activators. We optimized compound activity by synthesis and screening of structurally related analogs. The most potent analogs were characterized and shown in proof-of-concept studies to be of potential therapeutic utility in secretory diarrhea and polycystic kidney disease.

Materials and Methods

Chemicals. Forskolin, 1-desamino-8-D-arginine vasopressin (dDAVP), isoproterenol, propranolol, cholera toxin (CTX), *Escherichia coli* heat-stable toxin (STa), cAMP, chlorophenylthio (CPT)-cAMP, and 3-isobutyl-1-methylxanthine (IBMX) were purchased from Sigma (St. Louis, MO). Dipyridamole and MK571 were purchased from BIOMOL Research Laboratories (Plymouth Meeting, PA). Zeocin, hygromycin, and G-418 (Geneticin) were obtained from Invitrogen (Carlsbad, CA), Roche (Indianapolis, IN), and Invitrogen, respectively. Small molecules for primary screening were purchased from ChemDiv (San Diego, CA), and analogs purchased from ChemDiv and Asinex (Winston-Salem, NC). The collection of 50,000 chemically diverse, drug-like small molecules of molecular size 250 to 450 Da was screened previously (Yangthara et al., 2007). Chemicals for synthesis were purchased from Sigma-Aldrich.

Cell Culture and Transfection. Fisher rat thyroid (FRT) cells expressing human wild-type CFTR and YFP-H148Q/I152L, with or without V_2R, were generated as described previously (Yangthara et al., 2007). FRT cells were cultured in F-12 modified Coon's medium (Sigma) supplemented with 10% fetal bovine serum (Hyclone, Logan, UT), 2 mM glutamine, 100 units/ml penicillin, 100 μg/ml streptomycin, 500 μg/ml zeocin, 350 μg/ml hygromycin, and 500 μg/ml G-418. CHO-K1 cells were cultured in Ham's F-12 Nutrient mix medium supplemented with 10% fetal bovine serum, 100 units/ml penicillin, and 100 μg/ml streptomycin. MDCK cells were cultured in Dulbecco's modified Eagle's medium and Earle's balanced salt solution medium supplemented with 5% fetal bovine serum, 2 mM glutamine, 0.11 mg/ml sodium pyruvate, 1.5 g/l $NaHCO_3$, nonessential amino acids, 100 units/ml penicillin, and 100 μg/ml streptomycin. T84 cells were maintained in Dulbecco's modified Eagle's medium/Ham's F-12 (1:1) medium containing 10% FBS, 100 units/ml penicillin, and 100 μg/ml streptomycin. All cells were grown at 37°C in 5% CO_2/95% air.

For transient transfections, CHO-K1 cells at ~80% confluence were transfected with cDNA encoding the hemagglutinin-tagged human β2-adrenergic receptor using Lipofectamine 2000 (Invitrogen) according to manufacturer's instructions. Twenty-four hours after transfection, the cells were trypsinized and plated onto a 24-well plate. Cells were used at 24 h after plating (48 h after transfection).

Fluorescence Assay for cAMP Modulators. Transfected FRT cells were plated on black 96-well plates with clear plastic bottoms (Costar; Corning Life Science, Acton, MA), cultured overnight to confluence, washed three times with PBS, and treated with test compounds in a final volume of 60 μl. YFP-H148Q/I152L fluorescence was measured using a commercial plate-reader (FluoStar Optima; BMG Labtech, Winooski, VT) equipped with custom excitation and emission filters (500 nm and 544 nm, respectively; Chroma Technology Corp., Brattleboro, VT). Fluorescence in each well was measured for a total of 14 s. Two seconds after the start of data collection for each well, 100 μl of PBS/I^- (PBS with 100 mM Cl^- replaced by I^-) was injected into the well by a syringe pump. The compound library for screening contained 50,000 chemically diverse, drug-like small molecules. Stock compounds were stored in 96-well plates at 2.5 mM in DMSO. Compounds occupied 80 wells; the remaining 16 wells contained only DMSO to be used for positive and negative controls. Screening was done using an automated apparatus (Beckman Coulter, Fullerton, CA) containing a CO_2 incubator, carousels for compound plates and pipette tip boxes, plate washer (ELx405; BioTek Instruments, Winooski, VT), liquid handling station (Biomek FX; Beckman Coulter), and plate readers (FluoStar Optima). Robotic operations were control by SAMI software (version 3.3; Beckman Coulter).

For high-throughput screening, cells expressing human wild-type V_2R were plated in 96-well plates using a Multidrop Dispenser (Thermo Fisher Scientific). After overnight growth to reach confluence, cells were washed with PBS, and dDAVP (1 nM; Ferring Pharmaceuticals) was added together with test compounds (20 μM). The first and last columns of each plate were used for positive (PBS) and negative (dDAVP; no test compound) controls. I^- influx was assayed as described above after a 30-min incubation at 37°C with 95% CO_2/5% air. I^- influx ($d[I^-]/dt$ at $t = 0$) was computed from fluorescence time course data as described previously (Muanprasat et al., 2004). Percentage inhibition was computed as: % inhibition = 100 × (negative control − compound)/(negative control − positive control). Positive and negative control values denote $d[I^-]/dt$ obtained from the first and last columns of each plate, respectively. Primary screening data were subjected to histogram analysis for "hit" selection.

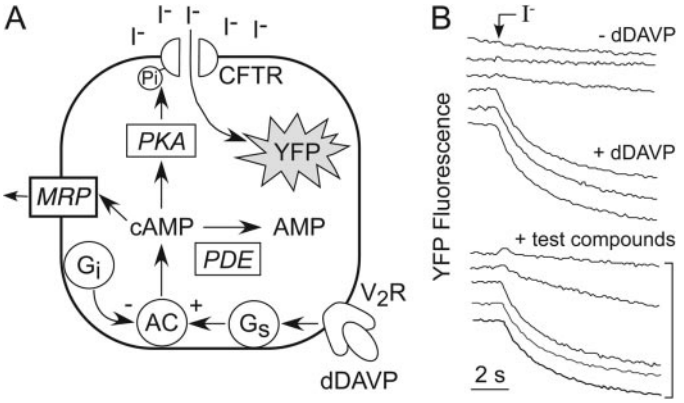

Fig. 1. "Pathway" assay and primary screening. A, principle of the assay showing activation of CFTR chloride channels and consequent iodide influx and YFP fluorescence quenching after dDAVP binding to the V_2R. B, representative original fluorescence data obtained from the primary screen. Control groups (top and middle) were incubated for 30 min without or with 1 nM dDAVP as indicated. Test compounds (bottom) were coincubated with dDAVP for the same time period. The tracings show two active and three inactive compounds. Iodide (I^-) was added where indicated.

Synthesis Procedures. Thin-layer chromatography was performed on Merck aluminum sheets containing silica gel 60 F_{254}. ^1H NMR spectra were recorded on a 400 MHz spectrometer (Varian, Inc., Palo Alto, CA) using tetramethylsilane as internal standard. Liquid chromatography and electrospray mass spectral data were performed on an integrated liquid chromatograph/mass spectrometer (Waters, Milford, MA).

Methyl (*E/Z*) 2-cyano-3-tolyl-pent-2-enoate (3). Methyl cyanoacetate (0.5 g, 0.0033 mol) and 4′-methylpropriophenone (0.33 g, 0.0033 mol) were dissolved in dry benzene (20 ml) to which ammonium acetate (0.051 g, 0.00067 mol) and acetic acid (0.2 ml) were added. The mixture was refluxed azeotropically using a Dean-Stark apparatus until water formation ceased. The reaction mixture was cooled, dried over sodium sulfate, and concentrated in vacuo. The residue was purified by flash chromatography (silica gel, hexane: EtOAc) to afford a pale yellow oil (yield 72%). ^1H NMR (400 MHz,

$CDCl_3$): 7.35 to 6.8 (m, arom-H, 8H), 3.84 to 3.64 (2s, -OCH_3, 6H, *Z*/*E*), 3.08 to 2.83 (2q, -CH_2, 4H, *E*/*Z*), 2.35 to 2.36 (2s, -CH_3 of tolyl. 6H), 1.03 to 1.02 (2t, -CH_3, 6H). ES-MS calculated for $^{12}C_{14}{}^{1}H_{15}{}^{14}N_1{}^{16}O_2$ *m*/*z* 229.2; found, *m*/*z* 230.

Methyl 2-amino-5-methyl-4-*p*-tolylthiophene-3-carboxylate (4). A stirred solution of methyl 2-cyano-3-tolyl-pent-2-enoate (0.2 g, 0.00087 mol) in a mixture of dry THF-MeOH (10 ml) was treated with sulfur (0.033 g, 0.0010 mol) and diethylamine (0.076 g, 0.108 ml, 0.00104 mol) at ambient temperature. The reaction mixture was stirred at 35–40°C until the starting material disappeared by thin-layer chromatography. The reaction mixture was concentrated in vacuo and the residue was purified by flash chromatography to afford product **4** as a pale yellow solid (yield 68%). ^{1}H NMR (400 MHz, $CDCl_3$): 7.11 (d, arom-H, 2H), 7.03 (d, arom-H, 2H), 5.82 (bs, -NH_2, D_2O exchangeable), 3.45 (s, -OCH_3, 3H), 2.34 (s, *p*-tolyl, 3H), 2.00 (s, -CH_3, 3H). ES-MS calculated for $^{12}C_{14}{}^{1}H_{15}{}^{14}N_1{}^{16}O_2S$ *m*/*z* 261.3; found, *m*/*z* 262. ES-MS calculated for $^{12}C_9{}^{1}H_{10}{}^{16}O_3$ *m*/*z* 166.06; found, *m*/*z* 167.

***exo*-Bicyclo[2.2.1]heptane-2,3-dicarboxylic anhydride (6)**. *exo*-Bicycyclo[2.2.1]hept-5-ene-2,3-dicarboxylic anhydride (1 g, 0.006 mol) was dissolved in dry THF (45 ml) and placed in a standard Parr bottle. Palladium (5%) on charcoal (~ 100 mg) was added and hydrogenation was carried out at 2.2 bar until H_2 uptake ceased. The catalyst was removed by filtration, the reaction mixture was concentrated under reduced pressure and petroleum ether and hexane were added to obtain product **6** as a crystalline white solid (yield 96%). Melting point, 78–79°C; ^{1}H NMR (400 MHz, $CDCl_3$): 2.90 (s, -CH, 2H), 2.84 (s, -CH, 2H), 1.25 to 1.78 (m, -CH_2, 6H). ES-MS calculated for $^{12}C_9{}^{1}H_{10}{}^{16}O_3$ *m*/*z* 166.06; found, *m*/*z* 167.

3-(3-(Methoxycarbonyl)-5-methyl-4-p-tolylthiophen-2-ylcarbamoyl)endo-bicyclo[2.2.1]heptane-2-carboxylic acid (7). A mixture of methyl 2-amino-5-methyl-4-*p*-tolylthiophene-3-carboxylate and *endo*-bicyclo[2.2.1]heptane-2,3-dicarboxylic anhydride were heated to melting to give crude product **7**. The mixture was dissolved in a minimum quantity of chloroform and crystallized in hexane/chloroform (yield, 56–60%). Melting point, 185–187°C; ^{1}H NMR (400 MHz, $CDCl_3$): 11.30 (bs, -COOH, 1H), 7.15 (d, arom-H, 2H), 7.01 (d, arom-H, 2H), 3.50 (s, -$COOCH_3$, 3H), 3.24 (d, -CH, 1H), 3.02 (d, -CH, 1H), 2.65 (d, -CH, 2H), 2.39 (s, *p*-tolyl, 3H), 2.11 (s, -CH_3, 3H), 1.4 to 1.8 (m, -CH_2, 6H). ES-MS calculated for $^{12}C_{23}{}^{1}H_{125}{}^{14}N_1{}^{16}O_5S$ *m*/*z* 427.15; found, *m*/*z* 428.

3-(3-(Methoxycarbonyl)-5-methyl-4-p-tolylthiophen-2-ylcarbamoyl)exo-bicyclo[2.2.1]heptane-2-carboxylic acid (8). A mixture of methyl 2-amino-5-methyl-4-*p*-tolylthiophene-3-carboxylate and *exo*-bicyclo[2.2.1]heptane-2,3-dicarboxylic anhydride were heated to melting to give crude product **8**. The mixture was dissolved in a minimum quantity of chloroform and precipitated with hexane (yield 56–60%). Melting point, 190–191°C; ^{1}H NMR (400 MHz, $CDCl_3$): 1.32 (bs, -COOH, 1H), 7.15 (d, arom-H, 2H), 7.02 (d, arom-H, 2H), 3.50 (s, -$COOCH_3$, 3H), 2.82 (dd, -CH, 1H), 2.68 (bs, -CH, 1H), 2.58 (bs, -CH, 1H), 2.38 (s, *p*-tolyl, 3H), 2.26 (d, -CH, 1H), 2.09 (s, -CH_3, 3H), 1.2 to 1.8 (m, -CH_2, 6H). ES-MS calculated for $^{12}C_{23}{}^{1}H_{125}{}^{14}N_1{}^{16}O_5S$ *m*/*z* 427.15; found, *m*/*z* 428.

Short-Circuit Current Measurements. Cells were cultured on Snapwell filters (Costar; Corning) until confluence (transepithelial resistance >500 Ω · cm). Apical membrane current was measured in an Ussing chamber (Vertical diffusion chamber; Costar) with Ringer's solution bathing the basolateral surface and half-Ringer's bathing the apical surface. The composition of Ringer's solution was: 130 mM NaCl, 2.7 mM KCl, 1.5 mM KH_2PO_4, 1 mM $CaCl_2$, 0.5 mM $MgCl_2$, 10 mM Na-HEPES, and 10 mM glucose, pH 7.3. Half-Ringer's solution was the same, except that 65 mM NaCl was replaced with Na-gluconate, and $CaCl_2$ was increase to 2 mM. The basolateral membrane was permeabilized with amphotericin B, as described previously (Ma et al., 2002). Chambers were bubbled continuously with air. Apical membrane current was measured using a DVC-1000 voltage-clamp apparatus (World Precision Instruments, Inc., Sarasota, FL).

Cyclic Nucleotide Assays. Cells were grown in 24-well plates, treated with test compounds, lysed by sonication, centrifuged to remove cell debris, and assayed for cAMP or cGMP according to manufacturer's instructions (Parameter cAMP or cGMP immunoassay kit; R&D Systems).

Intestinal Fluid Secretion. Mice (CD1 strain, 25–35 g) were deprived of food for 24 h but given 5% dextrose water. After anesthesia with tribromoethanol (Avertin) 250 to 400 mg/kg i.p., generally four mid-jejunal loops (20–30 mm each) were created using suture, as described previously (Ma et al., 2002). One hundred microliters of PBS containing CTX or STa (without or with test compound) was injected into the loops. The intestine was returned to the abdominal cavity and the incision closed with suture. The mice were allowed to recover from the surgery. Six hours later, the intestinal loops were removed, and net fluid accumulation quantified by measurement of weight-to-length ratio. Mice were euthanized by anesthetic overdose.

MDCK Cell Model of Polycystic Kidney Disease. MDCK cells were mixed with collagen (Purecol), MEM, 10 mM HEPES, pH 7.4, 100 units/ml penicillin, and 100 μg/ml streptomycin, and plated at 300 cells per well in 24-well plates, as described previously (Yang et al., 2008). After 2-h incubation in a CO_2 incubator at 37°C, cell culture media containing 1 μM forskolin was added on top of the cell-containing collagen gel. The media was changed twice daily. Small cysts developed by 4 days, at which time test compounds were added and the culture continued for 7 more days. Phase-contrast light micrographs were obtained every two days using a Nikon TE 2000-S inverted microscope (Nikon Corporation, Tokyo, Japan) at 20× magnification (546 nm, monochromatic illumination). Cyst growth was quantified using Image J software (http://rsbweb.nih.gov/ij/).

Results

Small-Molecule "Pathway" Screen. As diagrammed in Fig. 1A, our "pathway" screen detects increased cytoplasmic cAMP as an increase in CFTR-facilitated iodide influx, which results in fluorescence quenching of a cytoplasmic YFP-based halide sensor. A primary screen of 50,000 small molecules was done on FRT cells stably expressing human wild-type V_2R and CFTR, and the fluorescent halide sensor YFP-H148Q/I152L. The assay was designed to identify inhibitors of the V_2R-to-CFTR activation cascade that could target V_2R, G_s or G_i proteins, adenylyl cyclase, PDE, protein kinase A, cAMP efflux pathways [multidrug-resistance proteins (MRPs)], or CFTR.

Primary screening was done with the V_2R-selective vasopressin analog dDAVP (1 nM) and test compounds at 20 μM. Figure 1B shows the kinetics of YFP fluorescence in representative wells of 96-well plates. After 2 s for collection of baseline YFP fluorescence signal, iodide addition produced a slow reduction in fluorescence in the absence of dDAVP ("positive inhibitor" control) and a rapid reduction in dDAVP-treated cells ("negative inhibitor" control). Kinetic data for various test compounds are shown, the vast majority of which were inactive (bottom three curves). Of 50,000 compounds, three compounds were identified that reduced curve slope by more than 90% after iodide addition.

Synthesis of 2-(Acylamino)-3-thiophenecarboxylates. One class of active compounds that were found to suppress cyclic nucleotide concentrations, the 2-(acylamino)-3-thiophenecarboxylates, were resynthesized and characterized for use in subsequent biological assays. Figure 2A shows structures of two comparably active close analogs identified in the primary screen. Compounds were designated CNT_{inh} (cyclic nucleotide

inhibitor). Chemical synthesis of active compounds was achieved by the condensation of bicyclo[2.2.1]heptane-2,3-dicarboxylic anhydride with various 5-methyl-4-substituted aryl-3-alkoxycarbonyl-2-aminothiophenes. As a representative example, the strategy for synthesis of CNT_{inh}-03 is shown in Fig. 2B. The α,β-unsaturated nitrile **3**, isolated as an *E/Z*-isomeric mixture, was obtained by heating 4′-methyl propiophenone and methyl cyanoacetate in benzene using a Dean-Stark apparatus for constant water separation in the presence of glacial acetic acid and catalytic ammonium acetate. ^{1}H NMR of compound **3** showed a mixture of *E/Z* isomers with distinct singlets at 3.84 and 3.64 ppm, corresponding to the methyl group of the methyl esters, two quartets for the methylene group, and a multiplet for the remaining methyl and aromatic protons. Knoevenagel condensation product **3** was cyclized with sulfur and diethylamine to yield **4**. Condensation product **3** was converted to **4** when the reaction was carried out at 35–40°C, suggesting *E*-to-*Z* isomerization at elevated temperature. ^{1}H NMR confirmed a *para*-substituted aromatic ring, with a broad singlet of amine protons at 5.82 ppm. Three prominent singlets in the aliphatic region at 3.45, 2.34, and 2.00 ppm, corresponding to methyl ester, *p*-tolyl, and methyl protons, confirmed the formation of **4**.

To prepare the pure individual *exo* and *endo* isomers, the

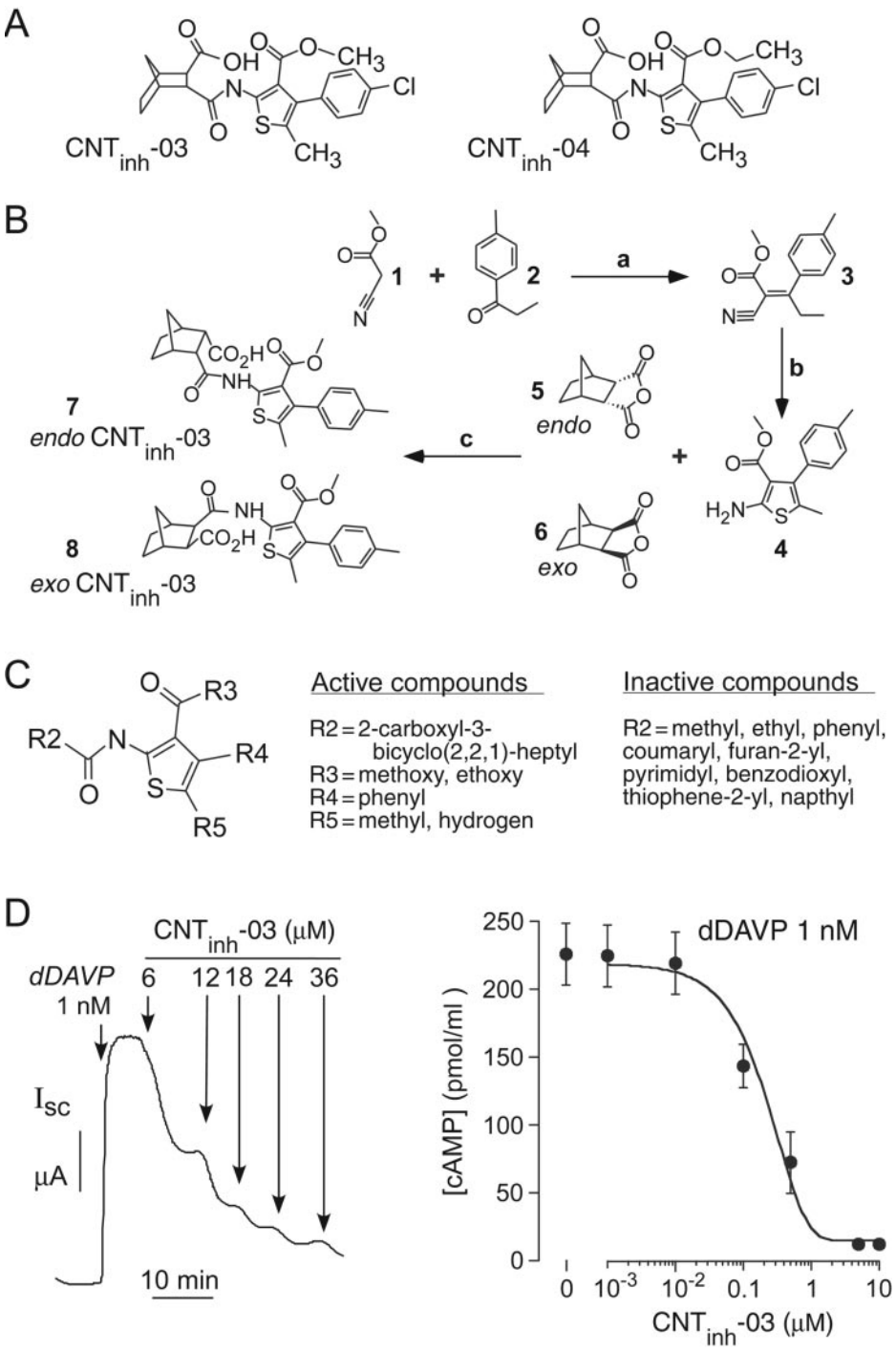

Fig. 2. Compound synthesis and structure-activity analysis. A, structures of CNT_{inh}-03 and CNT_{inh}-04. B, synthesis of CNT_{inh}-03. Reagents and conditions: (a) AcOH, NH_4OAc, C_6H_6 (azeotropic); (b) sulfur, Et_2NH, dry THF-MeOH, 35–40°C; (c) melt reaction. C, summary of structure-activity data obtained from screening of 124 analogs (see text for explanations). D, inhibition of short-circuit current (left) and cAMP (right) by CNT_{inh}-03 in FRT-V_2R cells after addition of 1 nM dDAVP. Cells were incubated with dDAVP and indicated concentrations of CNT_{inh}-03 for 20 min before cAMP assay. Data shown as mean ± S.E. (n = 3).

reactant *endo*-bicyclo[2.2.1]heptane-2,3-dicarboxylic anhydride was obtained commercially (melting point, 163°C) and the reactant *exo*-bicyclo[2.2.1]heptane-2,3-dicarboxylic anhydride, which was not available commercially, was synthesized by catalytic hydrogenation of *exo*-bicyclo[2.2.1]hept-5-ene-2,3-dicarboxylic anhydride. The *exo*-reactant had a very different melting point of 78–79°C, in agreement with literature data (Miklos et al., 2004). ^{1}H NMR of *endo*- and *exo*-bicyclo[2.2.1]heptane-2,3-dicarboxylic anhydride confirmed their structure, based on published data (Canonne et al., 1982). Condensation of **4** with *endo*- or *exo*-bicyclo[2.2.1]-heptane-2,3-dicarboxylic anhydride by a melt reaction yielded *endo*- and *exo*-CNT_{inh}-03, respectively.

Characterization and Structure-Activity Analysis of 2-(acylamino)-3-Thiophenecarboxylates. To establish structure-activity relationships, 124 synthetic analogs of CNT_{inh}-04 were screened in the functional assay. Table 1 summarized IC_{50} values for compounds of greatest interest, with data for additional active and other interesting compounds provided in the Supplemental Information. Figure 2C summarizes the structural features of the most active aryl-3-alkoxycarbonyl-2-(acylamino)thiophenes deduced from analysis of data from all compounds. The most active compounds contained *p*-tolyl, 3,4-dimethylphenyl, or ortho/para chlorophenyl substituents at R_4, methyl at R_5, methoxy or ethoxy at R_3, and 3-bicyclo[2.2.1]heptyl-2-carboxylic acid at R_2 of the thiophene nucleus. It is noteworthy that the *endo*- and *exo*-stereoisomers showed comparable potencies. As tabulated in Supplemental Information, the bicycloheptyl ring system at position R_2 could be substituted for various other nonaromatic multicyclic ring systems. Activity was abolished or substantially reduced with other substitutions at R_2, including *N*,*N*-dimethylaminomethyl, methyl, chloromethyl, 2-carboxyphenyl, mono-, di-, and trisubstituted nitrophenyl, substituted methoxyphenyl, 3-chlorobenzthiophenyl, pyridine-3-yl, coumaryl, tetrahydrofuryl, 1,4-benzodioxyl, substituted carboxy cyclohexenyl, substituted halophenyl, thiophene-2-yl, isoindolinyl-1,3-dione, anilino, and furanyl.

Figure 2D shows inhibition by CNT_{inh}-03 of chloride conductance (left) and cellular cAMP (right) in the V_2R and CFTR-expressing FRT cells used for primary screening. By short-circuit current analysis, the apparent IC_{50} for inhibition of CFTR chloride current after dDAVP stimulation was ~6 μM. Cellular cAMP was reduced to near zero with increasing CNT_{inh}-03. The reduced cytoplasmic cAMP concentration provides evidence against protein kinase A or CFTR as principle targets of CNT_{inh}-03.

Target Identification. Experiments were done to identify the cellular target of the 2-(acylamino)-3-thiophenecarboxylates. Figure 3A, left, shows that CNT_{inh}-03 was as effective as propranolol in reducing cAMP after isoproterenol stimulation in cells expressing β2-adrenergic receptors. Reduced cAMP was also found in CHO-K1 cells after forskolin or cholera toxin (Fig. 3A, middle and right). Reduced cAMP was also seen in various other cell lines (FRT, MDCK, T84) after agonist stimulation (data not shown). These results suggest the target of 2-(acylamino)-3-thiophenecarboxylate action is downstream of receptors and adenylyl cyclase, possibly by direct or indirect action on PDE(s). In support of action on PDEs was the finding that the 2-(acylamino)-3-thiophenecarboxylate suppressed cGMP levels in different cell types, as demonstrated in Fig. 3B in T84 cells after stimulation by STa toxin. Additional evidence supporting an action on PDEs was the finding that the nonselective PDE inhibitor IBMX (at 100 μM) partially abrogated the 2-(acylamino)-3-thiophenecarboxylate effect on cAMP suppression, as shown in several cell types such as CHO-K1 cells (Fig. 3C).

To test directly whether the 2-(acylamino)-3-thiophenecarboxylates act as PDE activators, short-circuit current measurements were done on CFTR-expressing FRT cells after permeabilization of the basolateral membrane and application to the basolateral bathing solution of low concentrations of cAMP or the relatively hydrolysis-resistant cAMP analog CPT-cAMP. Figure 3D shows stimulation of CFTR chloride current with added cAMP or CPT-cAMP (top and third curves). However, after pretreatment with CNT_{inh}-03, the increase in chloride current after cAMP was greatly reduced (second curve), whereas that after CPT-cAMP was not affected (fourth curve). These results provide evidence for in-

TABLE 1
Structure-activity relationships

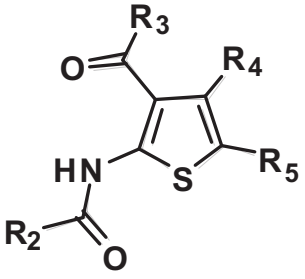

Compound	R_2	R_3	R_4	R_5	IC_{50}
					μM
CNT_{inh}-01	3-bicyclo[2.2.1]heptyl-2-carboxylic acid	OMe	2-Cl-phenyl	H	15
CNT_{inh}-02	3-bicyclo[2.2.1]heptyl-2-carboxylic acid	OMe	3,4-dimethyl-phenyl	Me	4
endo-CNT_{inh}-03	3-bicyclo[2.2.1]heptyl-2-carboxylic acid	OMe	4-methyl-phenyl	Me	4
endo-CNT_{inh}-04	3-bicyclo[2.2.1]heptyl-2-carboxylic acid	OEt	4-Cl-phenyl	Me	6
exo-CNT_{inh}-03	3-bicyclo[2.2.1]heptyl-2-carboxylic acid	OMe	4-methyl-phenyl	Me	4
exo-CNT_{inh}-04	3-bicyclo[2.2.1]heptyl-2-carboxylic acid	OEt	4-Cl-phenyl	Me	6
CNT_{inh}-05	3-bicyclo[2.2.1]heptyl-2-carboxylic acid	OEt	3,4-dimethyl-phenyl	Me	6

volvement of cAMP hydrolysis in compound action, suggesting direct or indirect action on PDEs.

One other possibility was considered as the target of CNT_{inh}-03 action—increased cellular cAMP efflux via plasma membrane pumps such as multidrug-resistance (MRP) proteins (Wielinga et al., 2003; Li et al., 2007). Evidence against this possibility is the generality of cAMP and cGMP suppression in multiple cell types. Furthermore, Fig. 3E shows that an inhibitor of MRP-mediated cAMP efflux, dipyridamole (Reid et al., 2003), did not affect CNT_{inh}-03 action. The lack of direct effect of dipyridamole on chloride current indicates that dipyridamole does not activate PDEs under the conditions of our experiments. Similar results showing no effect on CNT_{inh}-03 action were found for a different inhibitor of cAMP efflux, MK571 (20 μM) (data not shown).

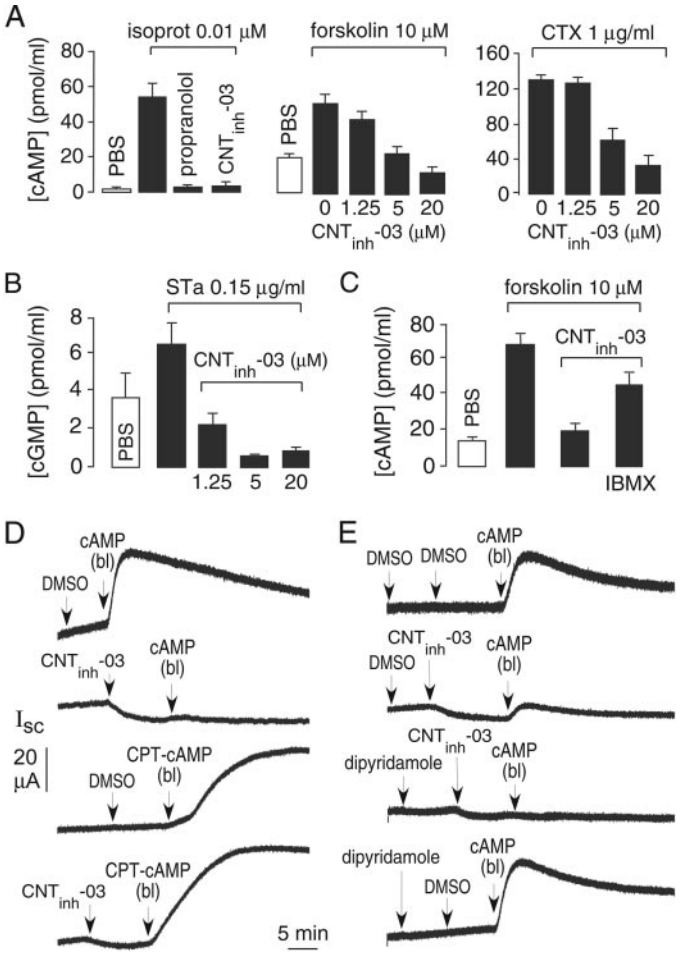

Fig. 3. Evidence for phosphodiesterase activation. A, left, reduction of cellular cAMP by 20 μM CNT_{inh}-03 in response to 0.01 μM isoproterenol (in β_2 receptor-expressing CHO cells). Cells were incubated with agonists/CNT_{inh}-03 for 20 min before assay. Propranolol was used at 20 μM. Middle, cAMP stimulated by 10 μM forskolin in CHO cells. Right, cAMP stimulated by 3 h incubation with 1 μg/ml cholera toxin (CTX). Data are mean ± S.E. (n = 3–5). B, reduction of cellular cGMP by CNT_{inh}-03 in response to 45-min incubation with 0.15 μg/ml STa toxin (SE, n = 4). C, IBMX abrogates cAMP suppression by CNT_{inh}-03, showing cellular cAMP in the absence and presence of 20 μM CNT_{inh}-03 / 100 μM IBMX as indicated. D, CNT_{inh}-03 inhibition of short-circuit current (Isc) in basolateral membrane-permeabilized FRT cells expressing human CFTR. As indicated, cells were incubated with 10 μM CNT_{inh}-03 (or DMSO vehicle), followed by addition of 20 μM cAMP or 8 μM CPT-cAMP in the basolateral (bl) bathing solution. E, experiments done as in D, except for pretreatment with 50 μM dipyridamole (or DMSO vehicle) before addition of 10 μM CNT_{inh}-03 (or DMSO vehicle), followed by 20 μM cAMP in the basolateral bathing solution. Experiments in D and E are representative of three similar sets of measurements.

Compound Efficacy in Models of Secretory Diarrhea and Polycystic Kidney Disease. As mentioned in the Introduction, there are several potential clinical applications of agents that reduce cyclic nucleotide concentration. Fluid secretion into the intestinal lumen in enterotoxin-mediated secretory diarrheas is produced by increased concentration of cyclic nucleotides in enterocytes, examples of which include cholera toxin causing elevated cAMP in cholera and STa toxin causing elevated cGMP in Traveler's (enteropathogenic *E. coli*) diarrhea (Field, 2003). Elevated cyclic nucleotide concentration activates CFTR, resulting in transcellular chloride secretion across the intestinal epithelium, which is followed by sodium and water secretion. T84 colonic epithelial cells are a commonly used human intestinal cell model of chloride secretion (Barrett, 1993). Figure 4A, left, shows slow activation of CFTR in T84 cells after cholera toxin. Short-circuit current was fully inhibited by CNT_{inh}-03. Figure 4A (right) shows an even greater potency of CNT_{inh}-03 for inhibition of short-circuit current after stimulation by STa toxin. These results are consistent with the data above showing reduced cAMP and cGMP concentrations in different cell types and with different agonists.

T84 cells develop large intracellular vacuoles at 3 h after cholera toxin exposure (Barkla et al., 1992; Crane et al., 2006), as shown in Fig. 4B. This change in morphology is thought to be caused by cAMP-dependent (though CFTR-independent) fluid secretion into intracellular vesicles. Figure 4B shows that CNT_{inh}-03 largely prevents the cholera toxin-induced vacuolarization in T84 cells, whereas CFTR chloride channel inhibition by $CFTR_{inh}$-172 does not.

We tested the efficacy of CNT_{inh}-03 in reducing intestinal fluid accumulation in a well established closed-loop mouse model of secretory diarrhea used extensively by our lab to evaluate the antisecretory properties of CFTR inhibitors (Thiagarajah et al., 2004). Intestinal loops were injected with saline, cholera toxin, or STa toxin, with or without CNT_{inh}-03. Intestinal loop fluid accumulation was quantified by loop weight-to-length ratio at 6 h. Figure 4C, left, shows that loop fluid accumulation increased greatly after cholera toxin and that the fluid accumulation was partially inhibited by CNT_{inh}-03. Figure 4C, middle, shows significant though lower stimulation of loop fluid accumulation by STa toxin compared with cholera toxin. CNT_{inh}-03 fully inhibited loop fluid accumulation after STa toxin. Figure 4C, right, shows that CNT_{inh}-03 did not affect intestinal fluid absorption, which is an important requirement for its potential application as an antidiarrheal.

Long-term elevation of cAMP in epithelial cells lining renal cysts is thought to be responsible for progressive cyst expansion in autosomal dominant polycystic kidney disease by stimulating epithelial cell proliferation and CFTR-dependent fluid transport into the cyst lumen (Mangoo-Karim et al., 1989). We used an established MDCK model of in vitro cyst formation (Yang et al., 2008) to test whether the 2-(acylamino)-3-thiophenecarboxylates could inhibit cyst growth. Figure 5A shows representative photographs of MDCK cell cysts over time after plating in a Matrigel matrix in the presence of forskolin. CNT_{inh}-03 remarkably reduced cyst expansion. Data from many individual cultures are summarized in Fig. 5B, as the ratio of final-to-initial cyst area. Although consid-

erable heterogeneity in cyst areas was seen, CNT_{inh}-03 clearly prevented the growth of large cysts. Figure 5C, left, summarizes the data as the percentage of total number of MDCK cells that formed cysts, as defined as structures with diameter >100 μm and having a lumen. CNT_{inh}-03 significantly reduced the percentage of MDCK cells that progress to form cysts. Figure 5C, right, confirmed that cAMP concentration was suppressed in forskolin-treated MDCK cells under the conditions of the cyst formation studies.

Discussion

The 2-(acylamino)-3-thiophenecarboxylates identified here are to our knowledge the first small-molecule general suppressors of cellular cyclic nucleotides. They reduced basal and agonist-induced elevation in cytoplasmic cAMP and cGMP concentrations in multiple cell types and in response to different types of agonists. Their mechanism of action seems to involve nonselective activation of PDEs, although we did not investigate whether they act direct or indirectly on PDEs. The compounds discovered here should be useful research tools in probing cyclic nucleotide signaling mechanisms, and notwithstanding specificity concerns, potentially for therapy of secretory diarrheas, polycystic kidney disease, and cAMP-dependent tumor growth. The strong PDE5/cGMP activating potency of 2-(acylamino)-3-thiophenecarboxylates also suggests their utility in preventing nitric oxide/cGMP-induced vasodilation, as in acutely antagonizing the actions of sildenafil or related PDE5 inhibitors.

Several lines of evidence suggested that the 2-(acylamino)-3-thiophenecarboxylates target PDEs. Both cAMP and cGMP were reduced in different cell types and in response to different agonists, including G protein-coupled receptor agonists, forskolin, CTX, and STa toxin. The 2-(acylamino)-3-thiophenecarboxylates abolished downstream cAMP action in response to added cAMP in permeabilized cells but not to the relatively hydrolysis-resistant analog CPT-cAMP. These and related experiments excluded a primary action of the compounds on GPCRs, G-proteins, adenylyl cyclase, protein kinase A, cyclic nucleotide cellular efflux, and CFTR. Further studies are needed to define compound selectivity to different PDE isoforms and the site of putative compound-PDE interaction. Such studies may present a considerable challenge because there are at least 11 PDE isoforms with extensive redundancy, cross-talk, and positive and negative feedback mechanisms and because the functions of several PDE isoforms remain incompletely understood (Bender and Beavo, 2006; Omori and Kotera, 2007). Further studies are also needed to determine whether compound action on PDEs is direct or indirect, perhaps acting though various kinases and/or phosphatases that modulate PDE activity.

Retrosynthetic analysis of CNT_{inh}-03 and CNT_{inh}-04 revealed the two important synthons as bicyclo[2.2.1]heptane-2,3-dicarboxylic anhydride (compounds **5** and **6**) and 5-methyl-4-substituted aryl-3-alkoxycarbonyl-2-aminothiophene (compound **4**). The Gewald synthesis is the most versatile method for the synthesis of the key synthon 5-methyl-4-substituted aryl-3-alkoxycarbonyl-2-aminothiophene, **4**, which was generated by a two-step procedure involving isolation of the α,β-unsaturated nitrile, **3**, from the Knoevenagel condensation of **1** and **2**. Subsequent conversion of the olefin, **3**, to the corresponding 2-aminothiophene, **4**, was accomplished by

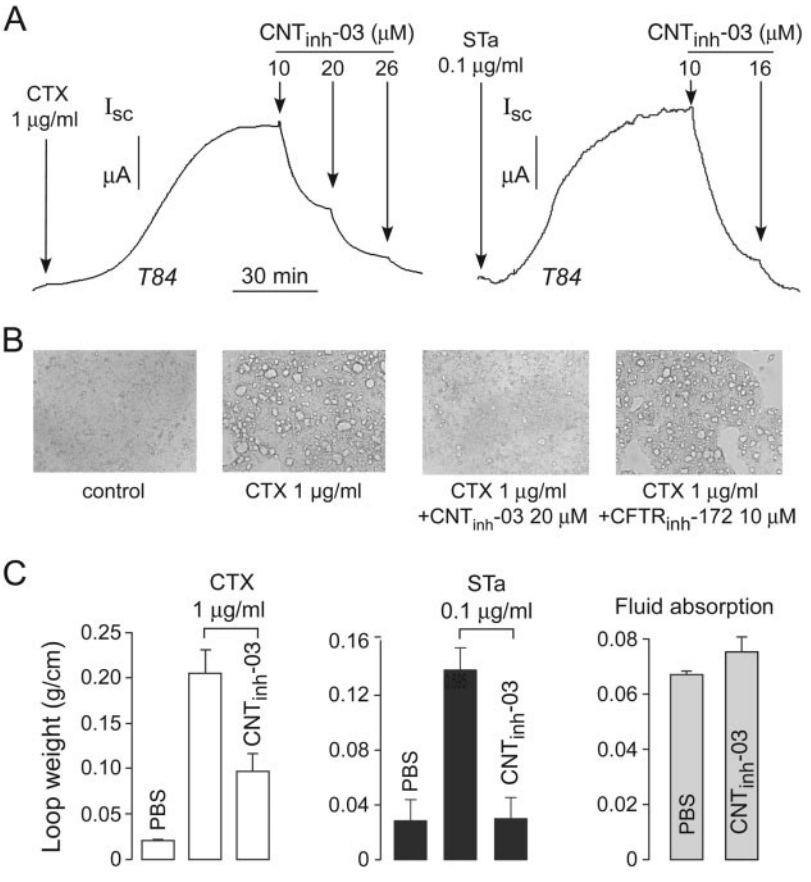

Fig. 4. Inhibition of fluid secretion in cell culture and mouse models of cholera and Traveler's diarrhea. A, short-circuit current measurements in T84 cells. CTX (left), STa (right), and CNT_{inh}-03 were added where indicated. B, intracellular vacuolization in T84 cells after CTX incubation for 3 h. Where indicated, CNT_{inh}-03 or $CFTR_{inh}$-172 were coincubated with CTX. C, fluid accumulation in closed intestinal loops in mice. Loops were injected with PBS, CTX (left), or STa (middle), without or with 20 μM CNT_{inh}-03. Loop fluid was assayed at 6 h in fluid secretion studies (left and middle) and at 20 min in fluid absorption study (right). Data shown as mean ± S.E. (n = 6–8 mice per condition).

treatment with sulfur and diethylamine. Condensation of 3-methoxycarbonyl-5-methyl-4-p-toyly-2-aminothiophene, **4**, with *endo-* or *exo*-bicyclo[2.2.1]heptane-2,3-dicarboxylic anhydride (compounds **5** and **6**) gave the *endo* and *exo* isomers of 3-methoxycarbonyl-5-methyl-4-p-toyly-2-aminothiophene bicyclo[2.2.1]heptane-2-carboxylic acid (compounds **7** and **8**). Structure-activity analysis of 124 analogs indicated 4-substituted aryl-3-alkoxycarbonyl-thiophen-2-ylcarbamoyl bicyclo[2.2.1]heptane-2-carboxylic acids as most potent cyclic nucleotide suppressors. It is noteworthy that we found little stereo-specificity in compound activity, allowing replacement, with minimal loss of function, of the bicycloheptane moiety with various other multicyclic moieties.

Proof-of-concept experiments support the potential utility of 2-(acylamino)-3-thiophenecarboxylates in reducing intestinal fluid accumulation in secretory diarrheas and slowing renal cyst growth and fluid accumulation in polycystic kidney disease. In response to cholera and STa toxins, the 2-(acylamino)-3-thiophenecarboxylates inhibited short-circuit current in T84 cells, a commonly used model of intestinal chloride secretion. In vivo, the 2-(acylamino)-3-thiophenecarboxylates reduced fluid accumulation in closed intestinal loops in mice at 6 h during continuous toxin exposure. PDE activation represents a novel strategy to reduce intestinal fluid secretion, which adds to the list of antisecretory mechanisms in clinical development, including CFTR and encephalinase inhibitors (reviewed in Thiagarajah and Verkman, 2005). The 2-(acylamino)-3-thiophenecarboxylates also slowed cyst growth and fluid accumulation in an in vitro MDCK model of polycystic kidney disease. Other antisecretory strategies under consideration for reducing fluid influx into renal cysts in polycystic kidney diseases include V_2R antagonism (Torres, 2008) and CFTR inhibition (Yang et al., 2008). Small-molecule PDE activators thus provide an alternative to therapies under development for secretory diarrheas and polycystic kidney disease.

In conclusion, the 2-(acylamino)-3-thiophenecarboxylates identified here, which seem to function as nonselective PDE activators, permit pharmacological suppression of cyclic nucleotides in cells and tissues. Potential applications of this compound class in reducing intestinal fluid secretion and renal cell cyst expansion were demonstrated. However, because PDEs are ubiquitously expressed, considerable further development is needed to achieve PDE isoform selectivity and selective organ/cell targeting.

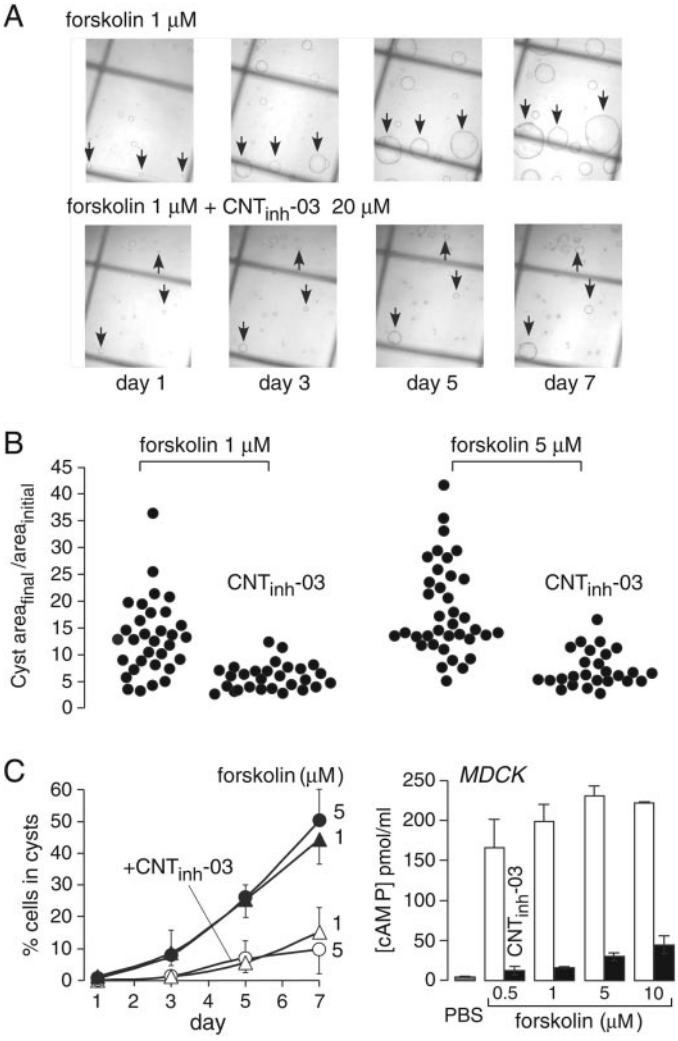

Fig. 5. Inhibition of MDCK cell cyst formation and expansion as a model of polycystic kidney disease. A, MDCK cells were cultured in a collagen matrix and exposed for 7 days to 1 μM forskolin (top) or 1 μM forskolin together with 20 μM CNT_{inh}-03 (bottom). Arrows point to developing cysts. B, cysts growth rates. Growth rates determined for individual cysts from cyst area at day 7 divided by initial cyst area at day 1 (Cyst $area_{final}/area_{initial}$). Each closed circle represents one cyst. C, left, percentage of MDCK cells that developed into cysts. MDCK cells were treated for 7 days with forskolin (1 or 5 μM), without or with 20 μM CNT_{inh}-03. Data shown as mean ± S.E. (n = 4 sets of cultures). Right, cAMP concentration in MDCK cells incubated with indicated concentrations of forskolin, without or with 20 μM CNT_{inh}-03 (SE, n = 4).

References

Barkla DH, Whitehead RH, and Hayward IP (1992) Effects of cholera toxin on human colon carcinoma cell lines. *Pathology* **24:**296–301.

Barrett KE. (1993) Positive and negative regulation of chloride secretion in T84 cells. *Am J Physiol* **265:**C859–C868.

Bender AT and Beavo JA (2006) Cyclic nucleotide phosphodiesterases: molecular regulation to clinical use. *Pharmacol Rev* **58:**488–520.

Canonne P, Belanger D, and Lemay G (1982) Novel synthesis of five- and six-membered spiro g-lactones in rigid bicyclic systems. *J Org Chem* **47:**3953–3959.

Crane JK, Choudhari SS, Naeher TM, and Duffey ME (2006) Mutual enhancement of virulence by enterotoxigenic and enteropathogenic *Escherichia coli*. *Infect Immun* **74:**1505–1515.

Field M (2003) Intestinal ion transport and the pathophysiology of diarrhea. *J Clin Invest* **111:**931–943.

Li C, Krishnamurthy PC, Penmatsa H, Marrs KL, Wang XQ, Zaccolo M, Jalink K, Li M, Nelson DJ, Schuetz JD, et al. (2007) Spatiotemporal coupling of cAMP transporter to CFTR chloride channel function in the gut epithelia. *Cell* **131:**940–951.

Ma T, Thiagarajah JR, Yang H, Sonawane ND, Folli C, Galietta LJ, and Verkman AS (2002) Thiazolidinone CFTR inhibitor identified by high throughput screening blocks cholera toxin-induced intestinal fluid secretion. *J Clin Invest* **110:**1651–1658.

Mangoo-Karim R, Uchic M, Lechene C, and Grantham JJ (1989) Renal epithelial cyst formation and enlargement in vitro: dependence on cAMP. *Proc Natl Acad Sci U S A* **86:**6007–6011.

Meyer G, Guizzardi F, Rodighiero S, Manfredi R, Saino S, Sironi C, Garavaglia ML, Bazzini C, Bottà G, Portincasa P, et al. (2005) Ion transport across the gall bladder epithelium. *Curr Drug Targets Immune Endocr Metabol Disord* **5:**143–151.

Miklos F, Hetenyi A, Sohar P, and Stajer G (2004) Preparation and structure of di-exo-condensed norbornane heterocycles. *Monatsh Chem* **135:**839–847.

Muanprasat C, Sonawane ND, Salinas D, Taddei A, Galietta LJ, and Verkman AS (2004) Discovery of glycine hydrazide pore occluding CFTR inhibitors: mechanism, structure-activity analysis, and in vivo efficacy. *J Gen Physiol* **124:**125–137.

Murakami M, Kamiya Y, Yanagita Y, and Mori M (1999) Gs alpha mutations in hyperfunctioning thyroid adenomas. *Arch Med Res* **30:**514–521.

Murthy KS (2006) Signaling for contraction and relaxation in smooth muscle of the gut. *Annu Rev Physiol* **68:**345–374.

Omori K and Kotera J (2007) Overview of PDEs and their regulation. *Circ Res* **100:**309–327.

Reid G, Wielinga P, Zelcer N, De Haas M, Van Deemter L, Wijnholds J, Balzarini J, and Borst P (2003) Characterization of the transport of nucleoside analog drugs by the human multidrug resistance protein-MRP4 and MRP5. *Mol Pharmacol* **63:**1094–1103.

Rybalkin SD, Yan C, Bornfeldt KE, and Beavo JA (2003) Cyclic GMP phosphodiesterase and regulation of smooth muscle function. *Circ Res* **93:**280–291.

Sack DA, Sack RB, Nair GB, and Siddique AK (2004) Cholera. *Lancet* **363:**223–233.

Sweeney WE Jr and Avner ED (2006) Molecular and cellular pathophysiology of autosomal recessive polycystic kidney disease (ARPKD). *Cell Tissue Res* **326:**671–685.

Thiagarajah JR, Broadbent T, Hsieh E, and Verkman AS (2004) Prevention of toxin-induced intestinal ion and fluid secretion by a small-molecule CFTR inhibitor. *Gastroenterology* **126:**511–519.
Thiagarajah JR and Verkman AS (2005) New drug targets for cholera therapy. *Trends Pharmacol Sci* **26:**172–175.
Torres VE (2008) Vasopressin antagonists in polycystic kidney disease. *Semin Nephrol* **28:**306–317.
Vaandrager AB (2002) Structure and function of the heat-stable enterotoxin receptor/guanylyl cyclase C. *Mol Cell Biochem* **230:**73–83.
van Staveren WC, Detours V, Dumont JE, and Maenhaut C (2006) Negative feedbacks in normal cell growth and their suppression in tumorigenesis. *Cell Cycle* **5:**571–572.
Wielinga PR, van der Heijden I, Reid G, Beijnen JH, Wijnholds J, and Borst P (2003) Charcaterization of the MRP4- and MRP5-mediated transport of cyclic nucleotides from intact cells. *J Biol Chem* **278:**17664–17671.
Yang B, Sonawane ND, Zhao D, Somlo S, and Verkman AS (2008) Small-molecule CFTR inhibitors slow cyst growth in polycystic kidney disease. *J Am Soc Nephrol* **19:**1300–1310.
Yangthara B, Mills A, Chatsudthipong V, Tradtrantip L, and Verkman AS (2007) Small-molecule vasopressin-2 receptor antagonist identified by a G-protein coupled receptor "pathway" screen. *Mol Pharmacol* **72:**86–94.

Address correspondence to: Dr. Alan S. Verkman, 1246 Health Sciences East Tower, Box 0521, University of California, San Francisco, San Francisco, CA 94143-0521. E-mail: alan.verkman@ucsf.edu